Offprint from

Proceedings of the 15th International Symposium on

Rarefied Gas Dynamics

June 16–20, 1986 Grado, Italy

Volume I

Edited by
Prof. Dr. Vinicio Boffi, University of Bologna, Italy
Prof. Dr. Carlo Cercignani, University of Milano, Italy

B. G. Teubner Stuttgart 1986

NONLINEARITIES IN THE INTERSPECIES TRANSFER OF MOMENTUM AND ENERGY FOR DISPARATE-MASS GAS MIXTURES AND SHOCK WAVE STRUCTURE

P. Riesco-Chueca, R. Fernandez-Feria and J. Fernandez de la Mora*

ABSTRACT

The large mass ratio m_p/m in a binary mixture of monoatomic gases is exploited to obtain expressions for the interspecies transfer of momentum and tensorial energy, valid for arbitrary values of the slip velocity. Self-collision integrals for the heavy gas are obtained by using a realistic model for the distribution function. The resulting formulation is applied to examine the internal structure of a normal shock wave in a disparate-mass gas mixture by means of a hypersonic and a near-equilibrium closure for the heavy and the light gas, respectively. In agreement with He/Xe experiments a double hump structure is observed here for the density profiles of the light gas. The evolution of the pressure tensor of the heavy gas is also followed across the shock. Using the magnitude of the heavy gas temperature overshoot as a measure of non-equilibrium, the influence of factors such as nonlinearity, molecular mass-ratio and density ratio on the departure from equilibrium is studied.

1. Introduction

Nonequilibrium phenomena arising in shock-waves of pure gases or gas mixtures in validate the use of hydrodynamic theories for the description of the shock structure. Different approaches have been used, such as the direct simulation Monte Carlo method developed by Bird [1], or, under special conditions, a continuum approach using two-fluid theories, which allow for large temperature and velocity differences between the species. In this case, exchange equations describing the energy and momentum transfer are required to couple the species. One possible choice is to model the interaction by adopting Maxwellian molecules leading to simple, but unrealistic transfer terms. The resulting equations are then solved for different asymptotic limits in the density ratio. [4] In this paper we follow Ref. [7], where the large mass disparity is used to obtain an expansion in the mass ratio for the interspecies transfer integrals. The result is a set of correlations for the cross-transfer terms, valid for the whole range of velocity and temperature differences between the species and therefore suitable to describe the shock-wave structure. Features such as the thickness of the wave and the heavy gas temperature overshoot are then obtained and compared to available data. Conclusions are drawn about the validity of the linearized expressions for the transfer terms.

2. Transfer terms

Consider the momentum and tensorial energy equations for the heavy species :

$$\partial_t(\rho_p U_p) + \nabla\cdot(P_p+\rho_p U_p U_p) = -\rho_p b \qquad (1)$$

$$\partial_t P_p + \nabla\cdot(2q_p + U_p P_p) + (P_p.\nabla)U_p + ((P_p\cdot\nabla)U_p)^T = -\rho_p(E + E_{self}). \qquad (2)$$

We shall follow the notation and results of Ref. [7], m, ρ, **U**, P being the molecular mass, density, mean velocity and stress tensor for the light gas, while the same notation with subscript p refers to the heavy gas. For the evaluation of the heterotransfer terms b and E, knowledge of the distribution functions f and f_p of both species and specification of the interaction potential is required. Rather than using an arbitrary approximation to the distribution functions, a rigorous expansion in powers of m/m_p is carried out to specify the distributions. Avoiding cases of extreme non-equilibrium, f is a Maxwellian to lowest order in m/m_p, while all the required information about f_p is the specification of the hydrodynamic quantities of the heavy gas. Once a model for the interaction potential is selected (Lennard-Jones in Ref.[7]), the cross-collision integrals are completely defined and can be evaluated numerically. These integrals have an analytic expression in two limits: for small velocity slip ($v = |U_p - U|/(2kT/m)^{1/2} \ll 1$) a linearization is carried out, whereas in the opposite limit the techniques of asymptotic integration are used. An optimal function can be fitted to match the numerical results between the two limits, resulting in simple correlations valid in the entire range of v.

To lowest order in m/m_p, the collision terms b, E in Eqs.(1-2) can be written as:

$$b = \delta \upsilon_B / \tau \qquad (3)$$

$$-E = 1/T\,[\Pi_1 \cdot (TI - T_p)]^S + \Pi_2 + 2m/m_p T\,(T_p \cdot \delta b)^S \qquad (4)$$

where $\delta = U_p - U$, $\Pi_1 = 2kT\,[\upsilon_B(I - e_3 e_3) + \upsilon_{\Pi 1} e_3 e_3]/\tau m_p$ and $\Pi_2 = Gm\delta^2 \upsilon_{\Pi 2}(I - 3e_3 e_3)/\tau m_p$. The temperature tensor is defined $T_p = m_p P_p / \rho_p k$ as usual. Note that the equilibrium closure for the light component permits to write the temperature tensor as TI . The superindex s denotes a symmetrized tensor : $A^S = 1/2\,(A + A^T)$ and the unit vector e_p points in the direction of the slip velocity δ. G and τ are constants given in terms of the Ω-integrals of the kinetic theory; however it is more convenient to express them in terms of the first approximation in Sonine polynomials of transport coefficients. For instance, τ is the usual relaxation time of linear theories, $\tau = Dm_p(n+n_p)/kTn$, where D is the first approximation in Sonine polynomials of the diffusion coefficient. The coefficients υ_B, $\upsilon_{\Pi 1}$, $\upsilon_{\Pi 2}$ contain the nonlinearities and they tend to unity as δ approaches zero. Only the expressions corresponding to the high temperature limit ($T \gg \varepsilon/k$,where ε is the depth of the Lennard-Jones well for the heavy-light interaction) are used here, since this is the relevant limit in most shock wave problems. For instance, ε/k takes the value 48.37k in the case of He/Xe mixtures; which is very small compared to the typical upstream temperature (~300k) and higher values reached across the shock.

The nonlinear factors υ_B, $\upsilon_{\Pi 1}$ and $\upsilon_{\Pi 2}$

$$\upsilon_B = (1 + 0.4596 v^2)^{1/3} \qquad (5)$$

$$\upsilon_{\Pi 1} = (1 + 2v^2 + v\,\partial \log \upsilon_B / \partial v)\,\upsilon_B \qquad (6)$$

$$\upsilon_{\Pi 2} = (1 + 0.312\, v^2)^{1/3} \qquad (7)$$

are plotted in Fig. 1, together with a more convenient approximation for $\upsilon_{\Pi 1}$, provided by the correlation

$$\upsilon'_{\Pi 1} = (1 + 1.34 v^{1.8})^{1/.675}.$$

The evaluation of the self-collision integrals E_{self} cannot be simplified by the above-mentioned mass-ratio expansion technique, so that specification of f_p is unavoidable. Nonequilibrium in problems with axial symmetry around the flow direction is

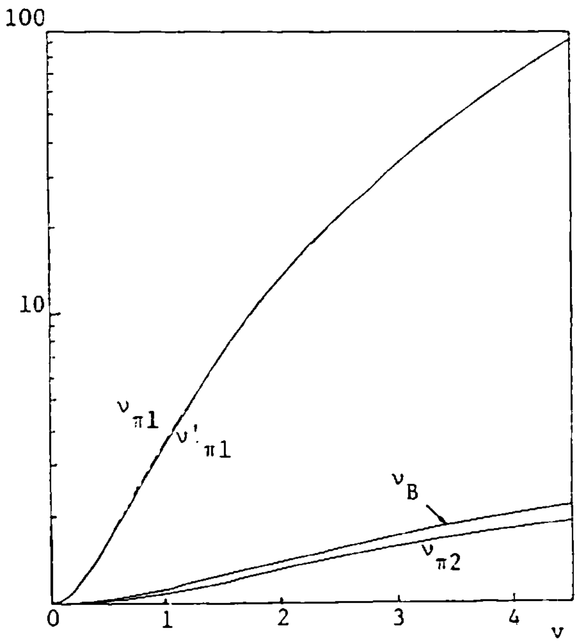

Fig. 1. Nonlinear factors as a function of v

generally accounted for by assuming an ellipsoidal Maxwellian (Gaussian) distribution with different parallel and perpendicular temperatures as parameters:

$$f_p = n_p\,(m_p/2\pi kT_{p||})^{1/2}\, m_p/2\pi kT_{p\perp} \exp(- m_p/2kT_{p||}(u_{p||}-U_p)^2 - m_p/2kT_{p\perp}u_{p\perp}^2), \quad (8)$$

Even though the range of situations where Eq.(8) is a realistic model for f_p is not well defined, possible inaccuracies arising from it will be shown to be unimportant, since cross-collision terms are dominant.

Using Eq. (8), E_{self} can be written as: [9], [10]

$$-E_{self} = n_p(m_p/2k)^{3/2}T_{p||}^{-1/2}T_{p\perp}^{-1}\int_0^1 (2kT_g/m_p)^{5/2}(3\eta^2-1)\Omega_{21}(T_g)d\eta\,(I-e_3e_3) \quad (9)$$

where $T_g = T_{p\perp}/(1-(T_{p||}-T_{p\perp})\eta^2/T_{p||})$ and Ω_{21} is defined in Hirschfelder et al .[5] The high temperature limit is again chosen so that the repulsive part of the Lennard-Jones potential prevails and Ω_{21} takes an analytic form which can be substituted in Eq.(9).

3. Governing equations

This paper deals with one-dimensional steady shock waves with density ratio of the heavy component up to order unity. Following reference [2], the mixture conservation equations can be written as

$$\rho U = \dot{m} \quad (10)$$

$$\rho_p U_p = \varepsilon\dot{m} \quad (11)$$

$$\rho U^2 + \rho_p U_p^2 + \rho kT/m - 4\mu/3\, dU/dx = P \quad (12)$$

$$\rho U(U^2/2+e) + \rho_p U_p\, U_p^2/2 + U(\rho kT/m - 4\mu/3\, dU/dx) - \lambda dT/dx = E, \quad (13)$$

where the heavy gas pressure tensor, heat flux and internal energy have been neglected with respect to their light gas counterparts, which are $0(m_p/m)$ larger. Additionally, a near equilibrium closure for the light component permits to express the pressure and heat flux terms as functions of the light gas velocity and temperature field. Strictly speaking, this closure is only uniformly valid across the shock for M close to unity. However, for the range of density ratios considered ($\varepsilon \leq 1$), the evolution in strong shock waves from upstream to downstream conditions takes place in two different scales. In the first one, light-light collisions are dominant and the light gas is compressed as in a pure gas shock wave. In the second scale a slower interspecies relaxation takes place and both species are compressed to the final state. Since most of the deceleration of the heavy gas takes place in this second scale, which is also the broadest one because of the mass disparity, the light gas hydrodynamic closure is used throughout the shock. Accordingly, results in the first scale will be only qualitative for strong shocks, but the remaining relaxation is realistically described. At the same time, the near-equilibrium assumption for the light gas permits to use the above described transfer terms and therefore close the problem.

Equations (10-13) are complemented with the following relaxation equations:

$$U_p\, dU_p/dx = b \quad (14)$$

$$k/m_p\,\{U_p(dT_{p\perp}/dx(I-e_3e_3)+dT_{p||}/dx\; e_3e_3\,)+2T_{p||}\, dU_p/dx\; e_3e_3\,\} = -E-E_{self}. \quad (15)$$

In Eqs.(14-15) the heavy gas pressure tensor and heat flux have been neglected because of the large mass disparity, which causes the heavy molecules to remain in hypersonic conditions across the shock.

The boundary conditions are, at $x \to -\infty$ $\rho = \rho_1$, $\rho_p = \varepsilon\rho_1$, $U = U_p = U_1$, $T = T_{p||} = T_{p\perp} = T_1$, while downstream the conditions are given by the Rankine-Hugoniot relations together with the condition of equilibrium: $x \to \infty$ $T = T_{p||} = T_{p\perp} = T_2$, $U = U_p = U_2$.

Introducing the dimensionless variables $\eta = U/U_1$, $\xi = U_p/U_1$, $\theta = T/T_1$, $\theta_\perp = T_{p\perp}/T_1$, $\theta_{||} = T_{p||}/T_1$, $\theta_p = (2\theta_\perp + \theta_{||})/3$, $ds = 3\dot{m}dx/4\mu$, Eqs. (10-15) become:

$$d\eta/ds = \eta - 1 + \varepsilon(\xi - 1) + 1/\gamma M^2 (\theta/\eta - 1) \tag{16}$$

$$[3/2Pr(\gamma - 1)M^2]d\theta/ds = -(\eta - 1)^2 + \varepsilon(\xi - 2\eta + 1)(\xi - 1) + 2[\theta + (\gamma - 1)\eta - \gamma]/\gamma(\gamma - 1)M^2 \tag{17}$$

$$\xi\, d\xi/ds = \theta(\eta - \xi)\upsilon_B/\eta F \tag{18}$$

$$\xi d\theta_\perp/ds = 2\theta/\eta F\,\{(\theta - \theta_\perp)\upsilon_B + Gv^2\theta\upsilon_{\Pi 2} + B\varepsilon\eta\,\theta_p^{11/6}\theta^{-1/3}(\theta_p - \theta_\perp)\upsilon_S/\xi\theta_{||}^{1/2}\theta_\perp\} \tag{19}$$

$$\xi\, d\theta_{||}/ds + 2\theta_{||}d\xi/ds = 2\theta/\eta F\,\{(\theta - \theta_{||})\upsilon_{\Pi 1} - 2G\upsilon^2\theta\upsilon_{\Pi 2} + 2\theta_{||}v^2\upsilon_B - 2B\varepsilon\eta\,\theta_p^{11/6}\theta^{-1/3}(\theta_p - \theta_\perp)\upsilon_S/\xi\theta_{||}^{1/2}\theta_\perp\}. \tag{20}$$

The dimensionless parameters Pr, F, B, G are functions of the Ω-integrals of the kinetic theory. Only the Ω-expression for G is given here:

$$G = 1/5\ \ \Omega^{(2,2)}/\Omega^{(1,1)} \tag{21}$$

where the Ω correspond to the cross interaction between light and heavy molecules . For the remaining parameters, an exact and more convenient representation is obtained by combining the first order approximation in Sonine polynomials of transport coefficients

$$Pr = \mu k\gamma/(\lambda(\gamma - 1)m)\quad ,\quad F = 3\gamma m_p M^2/4mSc\quad ,\quad B = \mu/2\mu_p Sc \tag{22}$$

where $Sc = \mu/[m(n + n_p)D]$, approximately uniform in the high temperature limit considered ($T >> \varepsilon/k$). B and G are evaluated at the upstream point $T = T_1$. For the high temperature limit the following values are obtained in the case of a He-Xe (He - Ar) mixture: $F = 18.52\ M^2$ ($7{,}215M^2$), $G = 0.4569$ and $B = 0.164$ (0.297). Alternatively, direct experimental values of μ, μ_p, D, can be inserted in Eqs. (21-22) to approximate F, B, and G. The fact that $B \ll 1$ shows that, when $\varepsilon < 1$, self-collisions are not dominant and therefore the choice of the model for f_p is not critical for the accuracy of the final results.

A particular feature of the system of differential equations (16-20) is that both the starting and ending points are singular. A direct numerical integration of the whole set is not feasible because of unstability problems. The first three equations are uncoupled so that the discussion on stability in Ref. [2] applies. In a second step, Eqs. (19-20) are solved to yield the heavy gas temperature tensor.

Eqs. (16-18) can be written in phase space

$$[(\eta - \xi)\upsilon_B\theta/\eta\xi F]\, d\eta/d\xi = \eta - 1 + \varepsilon(\xi - 1) + (\theta - 1/\eta)/\gamma M^2 \tag{23}$$

$$[3(\eta - \xi)\theta\upsilon_B/2\eta\xi F Pr(\gamma - 1)M^2]\, d\theta/d\xi = -(\eta - 1)^2 + \varepsilon(\xi - 1)(\xi - 2\eta + 1) + 2[\theta + (\gamma - 1)\eta - \gamma]/\gamma(\gamma - 1)M^2 \tag{24}$$

For weak shocks, the approximate conservation of entropy across the wave permits to reduce the number of equations and obtain a a numerically stable set [2]. When $M^2 - 1 \ll 1$ Eqs. (23-24) show that the small value of $F^{-1} << 1$ can be used to generate a perturbation solution. The lowest order outer solution, corresponding to the region where $d\eta/d\xi$, $d\theta/d\xi \lesssim 0(1)$ is obtained by neglecting the differential terms in Eqs. (23-24). An algebraic expression giving η, θ as functions of ξ can be easily deduced. The resulting formula corresponds to a two-fluid Euler-level in the broad relaxation region (outer scale) . Higher order approximations to the outer solutions can be readily obtained by using a regular perturbation scheme [2].

However, the assumption of small gradients is no longer valid in the starting region of the shock, where the light gas undergoes a shock, practically unaffected by the heavy component. In this region (inner scale) the upstream velocity of the heavy gas is approximately conserved ($\xi = 1$). Therefore taking η as independent variable, and expanding θ and ξ in Eqs. (23-24) as $\theta = \theta_0 + F^{-1}\theta_1 + \ldots$ and $\xi = 1 + F^{-1}\xi_1 + \ldots$, the resulting lowest order equations are obtained for the inner scale:

$$d\theta_0/d\eta = 2Pr\,(\gamma - 1)M^2\,[2(\theta_0 + (\gamma - 1)\eta - \gamma)/(\gamma(\gamma - 1)M^2) - (\eta - 1)^2] \\ /3[\eta - 1 + (\theta_0/\eta - 1)/\gamma M^2] \tag{25}$$

$$d\xi_1/d\eta = (\eta - 1)\, \upsilon_B \theta_0/[\eta(\eta - 1 + (\theta_0/\eta - 1)/\gamma M^2)]\,. \tag{26}$$

Eq. (25) is formally identical to the expression of a pure gas shock wave between the (η, θ) points (1,1) and (η_ℓ, θ_ℓ), where η_ℓ, θ_ℓ are the downstream Rankine-Hugoniot values for a pure gas, because setting $\xi = 1$ eliminates the influence of the heavy component. A backwards integraion starting at (η_ℓ, θ_ℓ) is required to avoid instabilities. On the other hand (η_ℓ, θ_ℓ) is also the limiting value of the algebraic external solution as $\xi \to 1$. Eq. (26) gives a first approximation to the breadth of the inner scale. Note that this function is singular at (η_ℓ, θ_ℓ). This feature permits to obtain the transition from the outer to the inner scale analytically by linearizing in $\theta - \theta_\ell$ and $\eta - \eta_\ell$. The following equations result:

$$d\eta^*/d\xi^* = (1 - 1/\gamma M_\ell^{\,2})\,\eta^* + \theta^*/\gamma M_\ell^{\,2} - \varepsilon\,\xi^*/\eta_\ell \tag{27}$$

$$d\theta^*/d\xi^* = 4Pr\,[(\gamma-1)\,\eta^* + \theta^* - \varepsilon(1-\eta_\ell)\gamma(\gamma-1)M_\ell^{\,2}\,\xi^*/\eta_\ell^{\,2}\,]\,/\,3\gamma \tag{28}$$

where M_l is the downstream Mach number for a pure gas shock wave with upstream Mach number M, and $\eta^* = (\eta - \eta_\ell)/\eta_\ell B$, $\theta^* = (\theta - \theta_\ell)/\theta_\ell B$, $\xi^* = (\xi - 1)/B$, with $B = (1-\eta_\ell)\nu_{B\ell}\theta_\ell/\eta_\ell F$ and $\nu_{B\ell} = \nu_B(\xi = 1, \eta = \eta_\ell)$. The complete solution takes the form:

$$\eta^* = \eta_p(\xi^*) + A\eta_1 e^{\lambda\xi^*} \tag{29}$$

$$\theta^* = \theta_p(\xi^*) + A\theta_1 e^{\lambda\xi^*} \tag{30}$$

where η_p, θ_p is a particular solution linear in ξ^* which can be interpreted as the local first correction to the lowest order downstream algebraic solution. Matching with this downstream algebraic solution is achieved automatically by rejecting the contribution from the nondecaying exponential and keeping only the exponential term associated to the other eigenvalue λ. (η_ℓ, θ_ℓ) is the corresponding normalized eigenvector, while the constant A can be determined numerically by matching with the solution of Eq. (17-18) as $\eta \to \eta_\ell$ and $\theta \to \theta_\ell$. The matching is carried out neglecting the algebraic term, so that A does not depend on ε. Some values of A are A= .84, 1.13, 1.25, 1.31, 1.34, 1.36, 1.38, 1.39, 1.40 for respective values of M=2, 3, 4 ,5 6, 7, 8, 9, 10. The resulting values of η, θ as a function of ξ are then substituted in Eqs.(18-20) to yield the heavy gas temperature tensor evolution and the complete structure in the physical plane.

Fig. 2 shows the results, using the above-outlined technique, for the density profiles of both species in a mixture of Xe in He. The conditions for this example are taken from the experiments of Gmurczyk et al [3]; this particular use has also been modeled by means of a modified BKG theory [6] and a numerical simulation [8] , with conflicting results. Fig. 2 shows the two-scale structure consisting of a sharp region where the light gas undergoes a pure gas shock wave, while the heavy component is approximately unaffected, together with a long tail where both species relax to the final equilibrium state. The values of μ used to integrate Eq.(18) are taken from Vargaftik [11]. Our results do not show the overshoot in the helium density profile reported in the experiments which is probably caused by measurement inaccuracies at the tail of the shock.

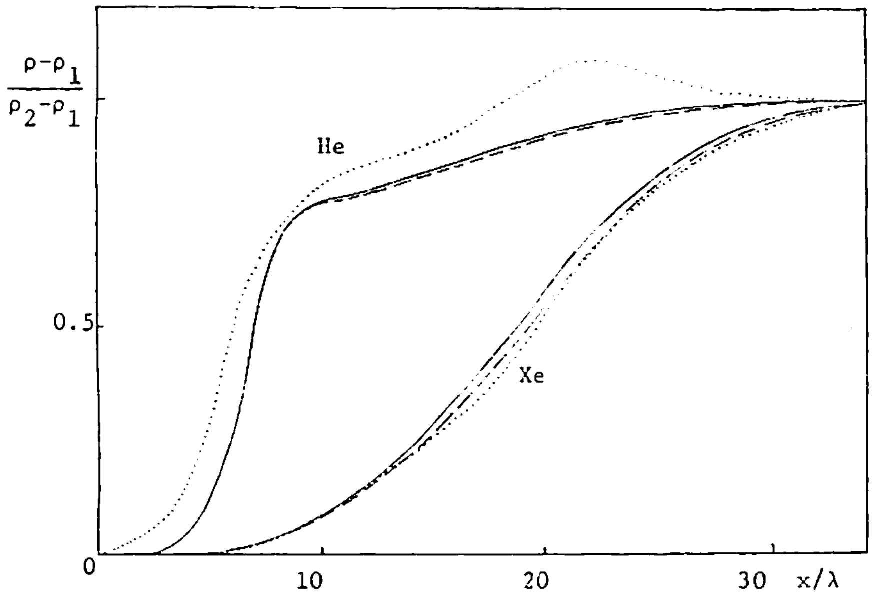

Fig. 2. Density profile for a He /Xe shock wave: ε = 1.014, M = 2.7828, λ = .46 mm (upstream mean free path). —— Analytic computation. -----Linearized solution. .... Gmurczyk experiments.

A two-step or double hump structure, which can be characterized by the occurrence of three inflection points (dent) in the density profile, instead of one, is apparent in the figure. The location of the first step approximately corresponds to the end point of the light species pure gas shock wave, $(1/\eta_\ell-1)/(1/\eta_2-1)$. The dent becomes less visible as the Xe concentration increases or the Mach number decreases, because this causes the two scales to merge. Good agreement exists with the experiments regarding the shock thickness (measured in units of upstream mean free paths of the mixture) [3]. A rough estimate for the breadth of the scales is given by $L_{inner} \sim \mu M/\rho U$ (self-collisions dominant) and $L_{outer} \sim U_1\tau_2$ (cross-collisions dominant), where τ_2 represents the downstream relaxation time $k_2m_p/Scmn_2kT_2$. If a 2/3 power dependence on the temperature for μ is assumed (high temperature limit) and the strong shock relations for T_2/T_1 and n_2/n_1 are used, the relation between the scales becomes

$$L_{outer}/L_{inner} = C\,(m_p/mSc)\,(M/(1+\varepsilon))^{1/3} \tag{31}$$

where C is a constant taking typically values one order of magnitude below unity. A generalized formula for a shock not in the strong limit would involve a more complex function of M and ε.

However Eq. (31) and the sequence of profiles in Fig. 3 illustrate the evolution of the thickness ratio. First, against what we might naively expect, this ratio is smaller than m_p/m (except for very large M), as shown in Fig. 3. Besides, the thickness ratio grows as M increases, and as the heavy gas dilution increases.

Figure 2 also includes the resulting profile when a linearized model for the collision terms is used ($\upsilon_{\Pi 1}=\upsilon_{\Pi 2}=\upsilon_B=\upsilon_S=1$, higher terms in v neglected). As can be observed, the difference is small, because the only nonlinear correction in Eq.(18) is υ_B which, for the most extreme case (very strong shock with $v \approx 1/(\gamma-1)^{1/2}$), takes the value 1.2 (see Fig.1) . Therefore, the linear approximation gives a good description of the density field. As will be shown in the next section, this is not the case for the temperature field.

Fig.3. Analytical density profiles for a He-Xe mixture with $\varepsilon = 0.5$ and different Mach numbers. $\frac{\rho-\rho_1}{\rho_2-\rho_1}$ ($\lambda' = 4\mu_1 M/3\dot{m}$)

-------- M=2

———— M=3

- · - · - · M=5

··············M=10

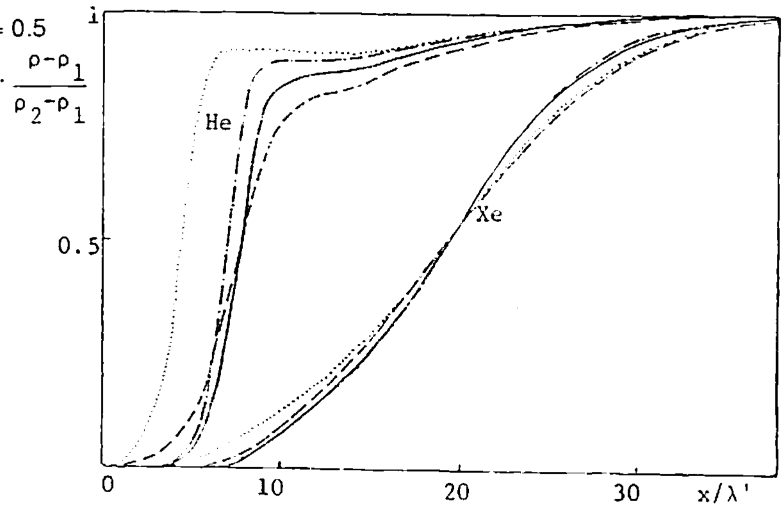

4. Structure of the temperature tensor

The evolution of the temperature components across the shock wave is governed by Eqs.(19,20) which clearly show the sources of temperature non-equilibrium. The parallel temperature rises as a consequence of compression heating ($-2\theta_{||}d\xi/ds$) and friction heating (power supplied by the drag force, $4\theta\theta_{||}\, v^2\upsilon_B/\eta F$). While these terms increase the nonequilibrium, the relaxation and self-collision terms bring the species closer to equilibrium. The final overshoot (Fig. 4.) in the parallel temperature results from the action of all these terms.

The importance of nonlinear heating in strong shocks is evident from the figure: the linearized solution is only valid for M below 1.2÷1.3. Note that the friction heating term is absent in a linearized theory. This, together with the above-mentioned balance determining the overshoot, explains the sensitivity of the heavy gas profile to the description of nonlinearities. Fig. 5 also includes the results obtained by Bird [1] using a Monte Carlo simulation (He-Ar, ε=1). His data,

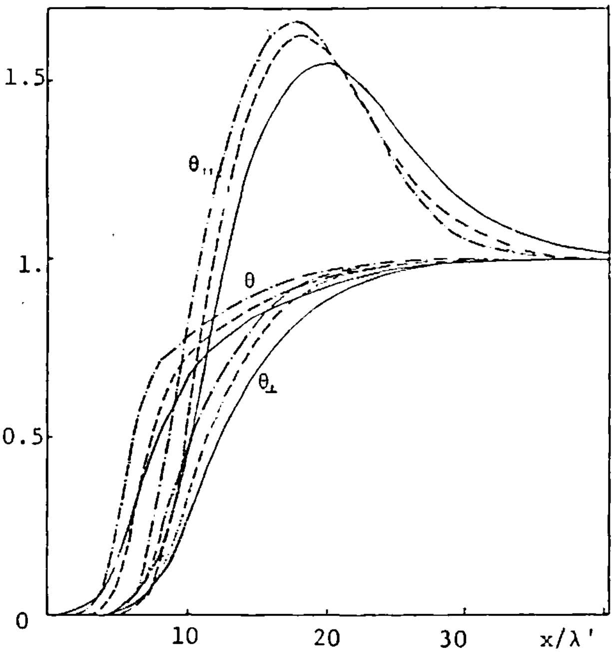

Fig. 4. Heavy and light gas temperature profiles (θ, $\theta_{||}$, $\theta_{\perp}$) in a ε=0.5 He-Xe mixture
——M=2, ------M=3, - · · · - M=5

originally a function of the mixture Mach number M_S [$M_S{}^2$=$M^2(1+\varepsilon)$], are here replotted as a function of the light gas Mach number M. Several differences are noticeable. According to Bird, overshooting takes place as soon as M_S>1. Our results on the contrary show that the overshoot exponentially decays to zero as M→1, at values larger than M_S=1. This is confirmed by the

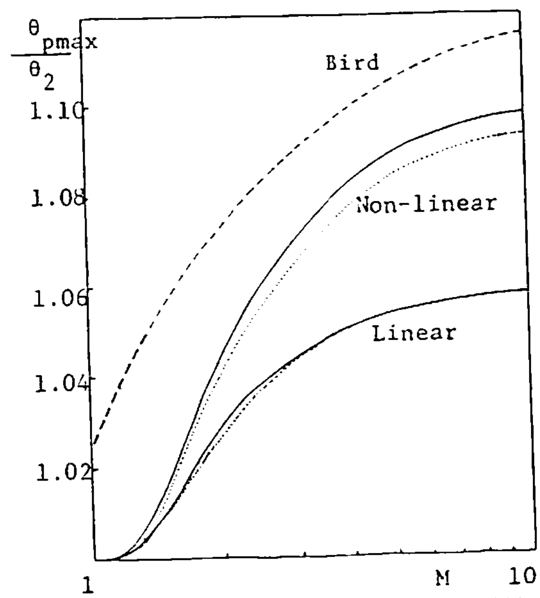

Fig. 5. Heavy gas temperature overshoot in ε=1 He-Xe (——) and He-Ar (············) mixtures
Bird's simulation for He-Ar: -----

coincident trend of the linearized equations close to M=1. An additional difference consists in the overall larger values for the overshoot obtained by Bird. However, the curves are qualitatively similar and both tend to a limiting value $\theta_{pmax}/\theta_2 \sim 1.1 \div 1.12$ as M gets large. The corresponding values for the parallel component of the heavy gas temperature are much larger (in the asymptote, $\theta_{||}/\theta_2 \approx 1.46$). The influence of the mixture mass-ratio can also be observed (overshooting increases with m_p/m). However our results are subject to the constraint of large m_p/m, so that they are less reliable in the case of He-Ar mixtures. An additional source of discrepancy with Bird might be the different interaction potential adopted.

Figure 6 shows the same curve in the case of a very dilute mixture (ε=0.0001) for He-Xe and He-Ar. The large increase in the overshoot with respect to the results for ε=1 is mainly due to the strong dependence of the light gas temperature profile on ε. The choice of the parameter represented (θ_{pmax}/θ_2) also causes an apparent magnification of the non-equilibrium as $\varepsilon \rightarrow 0$, because θ_2 drops down to θ_p. An additional, minor contribution to non equilibrium is provided by the absence of equilibrating heavy gas self-collisions when $\varepsilon \ll 1$. The same differences with the linearized approximation are patent. In this linear limit, the additional neglect of self-collision terms permits to obtain an explicit analytic expression for the heavy gas temperature tensor. The calculations are carried out assuming an instantaneous pure gas shock (η_ℓ, θ_ℓ) followed by a relaxation of the heavy species towards $(\eta_2, \theta_2)=(\eta_\ell, \theta_\ell)$. Defining $\mu=\xi-\eta$, $\mu_\ell = l-\eta_\ell$, the expressions for s, $\theta_{||}$ and $\theta_\perp$ are:

$$s = -\eta F(\mu-\mu_\ell+\eta \ln(\mu/\mu_\ell))/\theta \tag{32}$$

$$\theta_{||} = (\mu/\xi)^2 [1/\mu_\ell^2 - 2\theta[\ln \mu/\mu_\ell - 2\eta(1/\mu - 1/\mu_\ell) - \eta^2/2(1/\mu^2 - 1/\mu_\ell^2)] \tag{33}$$

$$\theta_\perp = \theta + (1-\theta)(\mu/\mu_\ell)^2 \tag{34}$$

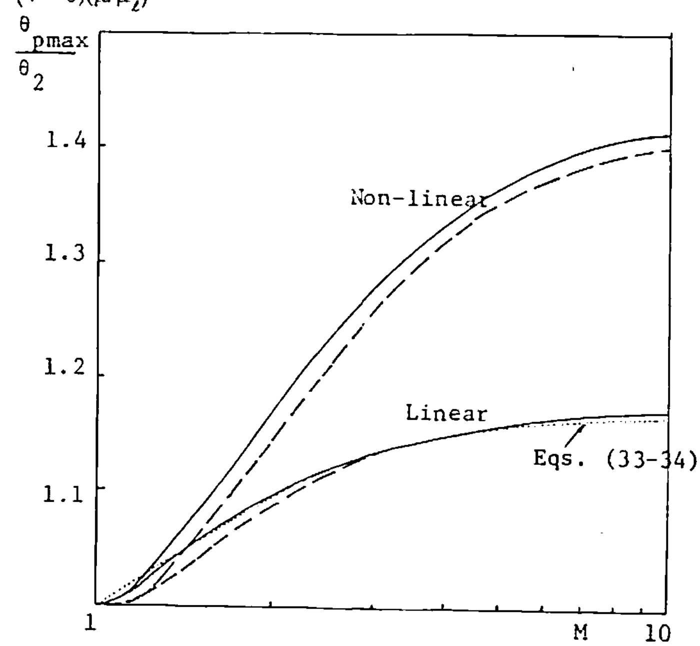

Fig. 6. Temperature overshoot in the dilute limit (ε=.0001).
——— He-Xe ------ He-Ar ············ Eqs. (32-34)

These functions are plotted in Fig. 6. The agreement with the numerically obtained linearized solution is good except for M ≈ 1 where the assumption of an independent an instantaneous pure gas shock is not realistic.

Acknowledgements.

Support from a cooperative grant from Schmitt Technologies Associates and the State of Connecticut (number 885-176) is gratefully acknowledged. One of the authors (P.R.Ch.) is sponsored by the US-Spanish Joint Committee For Cultural and Educational Cooperation.

References

[1] Bird, G.A. Rarefied Gas Dynamics. ed. H. Oguchi. University of Tokyo Press(1984)175.

[2]. Fernandez-Feria, R., Fernandez de la Mora, J. Shock wave structure in gas mixtures with large mass disparity. Submitted for publication to J. Fluid Mech.

[3]. Gmurczyk, A.S., Tarczynski, M., Walenta, Z.A. . Rarefied Gas Dynamics. v.1, ed. R. Campargue (1979) 333-334.

[4]. Harris, W.L.and Bienkowski, G.K., Phys. Fluids 14 (1971), 2652.

[5] Hirschfelder, J.O., Curtiss, C.F., Bird, R.B. Molecular Theory of Gases and Liquids. Wiley, New York (1954).

[6]. Platowski, T. Rarefied Gas Dynamics. v.1, ed. R. Campargue (1979) 323-331.

[7]. Riesco-Chueca, P., Fernandez-Feria, R., Fernandez de la Mora, J. Interspecies transfer of momentum and energy in disparate-mass gas mixtures. Phys. Fluids, to appear.

[8]. Schmidt, B., Seiler, F., Worner, M. J. Fluid Mech. 163, 305-326.

[9]. Takahashi, N. and Teshima, K., in Rarefied Gas Dynamics ed. H. Oguchi. U. of Tokyo (1984) 703-710

[10].Toennies, J.P. and Winkelmann, K. J. Chem. Phys. 66 (1977) 3965-3979.

[11]. Vargaftik, N.B., Tables on the Thermophysical Properties of Liquids and Gases, Wiley, New York, 1975

*Yale University, Mech. Eng. Department. Box 2159 Y.S., New Haven CT 06520-2159, U.S.A.